

Abrasive wear property of laser melting/deposited Ti₂Ni/TiNi intermetallic alloy

GAO Fei(高 飞), WANG Hua-Ming(王华明)

Laboratory of Laser Materials Processing and Manufacturing, School of Materials Science and Engineering,
Beihang University, Beijing 100083, China

Received 15 July 2007; accepted 10 September 2007

Abstract: A wear resistant intermetallic alloy consisting of TiNi primary dendrites and Ti₂Ni matrix was fabricated by the laser melting deposition manufacturing process. Wear resistance of Ti₂Ni/TiNi alloy was evaluated on an abrasive wear tester at room temperature under the different loads. The results show that the intermetallic alloy suffers more abrasive wear attack under low wear test load of 7, 13 and 25 N than high-chromium cast-iron. However, the intermetallic alloy exhibits better wear resistance under wear test load of 49 N. Abrasive wear of the laser melting deposition Ti₂Ni/TiNi alloy is governed by micro-cutting and plowing. Pseudoelasticity of TiNi plays an active role in contributing to abrasive wear resistance.

Key words: TiNi; Ti₂Ni; abrasive wear; intermetallic alloy

1 Introduction

TiNi alloys are extensively applied in mechanical, electric, chemical, aerospace and medical industries due to their excellent shape memory effect, pseudoelasticity, toughness, ductility and biocompatibility. The TiNi-based shape memory alloys exhibit excellent wear resistance due to their many superior properties, such as pseudo-elasticity, toughness and ductility[1–10]. Studies[1–3] in recent years indicate that stress-induced reversible martensitic transformation plays an active role in contributing to the wear resistance. The deformation within the pseudoelastic range is recoverable and this rubber-like property diminishes plastic deformation and retards crack propagation. The TiNi alloy with better pseudoelasticity exhibits higher wear resistance.

However, abrasive wear resistance of TiNi still needs to be improved due to the load-bearing capability and low hardness. The outstanding toughness and ductility make TiNi a promising candidate as the matrix for a wear resistant alloy. The wear resistance would be further enhanced if a TiNi matrix composite is fabricated by in-situ incorporation of hard intermetallic phase.

At present, Ti₅Si₃, Ti₂Ni₃Si, TiN, TiC, Ni₃Ti and

Ti₂Ni are selected to enhance the yield strength of TiNi[11–17]. The hard intermetallic compound Ti₂Ni (with microhardness of approximate HV700) is precipitated during the solidification process in both equal-molar and Ti-rich TiNi alloys[18–20]. The Ti₂Ni intermetallic compound has good combination of ductility because of its face-center-cubic crystal structure[14]. ISHIDA et al[21] indicated that TiNi alloy containing spherical precipitates Ti₂Ni exhibited higher yield stress. Therefore the intermetallic compound Ti₂Ni with face-center-cubic crystal structure is strongly expected to be a reinforcing phase for a TiNi matrix wear resistant composite due to its high hardness and strong atomic bonds.

In the present work, the TiNi intermetallic matrix in-situ composite reinforced by Ti₂Ni was designed and fabricated by the laser melting deposition. Abrasive wear resistance of the Ti₂Ni/TiNi alloy was evaluated, and the corresponding mechanism was discussed.

2 Experimental

Commercial pure Ti-Ni elemental powder blends in nominal chemical composition (molar fraction, %) of 53.8Ti-46.2Ni were selected as the raw material. Short

cylinder-shape ingots of $Ti_2Ni/TiNi$ alloy with an average diameter of 18 mm and height of 12–14 mm were fabricated by the laser melting deposition in a newly patented laser melting furnace[22]. The alloy powder delivering in an argon shielded water-cooled copper-mold was melted by a high-power laser beam from an 8 kW continuous-wave CO_2 laser, as shown in Fig.1. The laser deposition parameters are as follows: laser beam power 3 kW, laser beam diameter 14 mm, laser beam irradiation time 30–50 s.

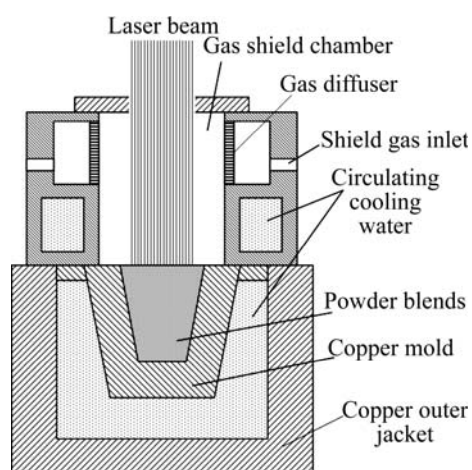


Fig.1 Schematic illustration of water-cooled copper-mold laser melting furnace

Metallographic sections were prepared using mechanical polishing procedures and were etched in $HF-HNO_3-H_2O$ water solution in volume ratio of 1:6:7 for approximately 5 s. The microstructure was characterized by KYKY 2800B and FEI Quanta6000 scanning electron microscope(SEM). X-ray diffraction (XRD) were conducted using the Rigaku D/max 2200 pc automatic X-ray diffractometer with $Cu K_{\alpha}$ radiation to identify the constitution phase. Phase chemical compositions were analyzed by energy dispersive spectroscopy(EDS) using Noran Ventage DSI spectrometer. Phase transition of $TiNi$ was studied with a NETZSCH DSC 404C differential scanning calorimeter. Thermogram was obtained over a temperature range of 40–200 °C with heating rate of 5 °C/min.

Abrasive wear behavior was examined by using an abrasive wear tester, schematically illustrated in Fig.2. Abrasive wear tests were carried out at room temperature by applying different loads of 7, 13, 25 and 49 N. SiC (approximately 40 μm) was selected as the abrasive particle and abrasive SiC paper was stuck on the disk. The samples were 6 mm in diameter. The test parameters were: sliding speed 0.5 m/s, wear test time 24 s and total wear sliding distance 12 m. Each test was repeated three times. Wear mass loss was measured using an electronic

balance (Sartorius BS110) with an accuracy of 0.1 mg. Wear mass loss was used to rank wear property of the test materials (the lower the wear mass loss, the higher the wear property). High-chromium cast-iron was selected as the reference material.

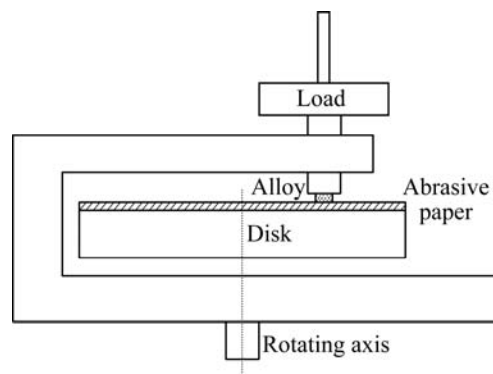


Fig.2 Schematic illustration of abrasive wear tester

3 Results

The laser melting/deposited $Ti_2Ni/TiNi$ intermetallic alloy has a dense and uniform structure. Microstructure of the alloy consists of primary dendrites and remained interdendritic matrix, as shown in Fig.3. Results of EDS analysis indicate that the primary dendrites are $TiNi$ and interdendritic phase is Ti_2Ni , which is qualitatively in good agreement with the phase predications of $Ti-Ni$ binary phase diagram, as shown in Fig.4.

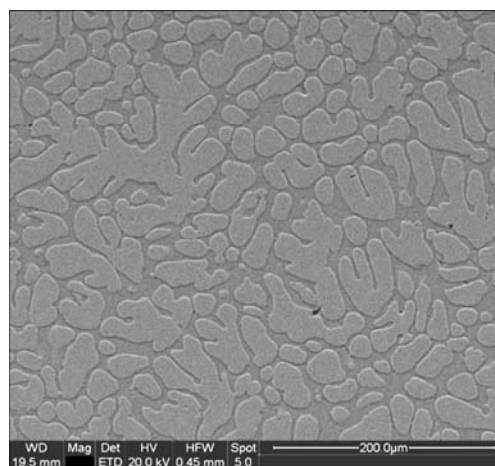


Fig.3 SEM micrograph showing microstructure of laser melting/deposited $Ti_2Ni/TiNi$ intermetallic alloy

Fig.5 shows wear mass loss of $Ti_2Ni/TiNi$ alloy and the reference material under different abrasive wear loads. Wear mass loss of the intermetallic alloys is more than that of the reference material under low abrasive wear loads of 7, 13 and 25 N. However, $Ti_2Ni/TiNi$ intermetallic alloy exhibits better wear resistance under

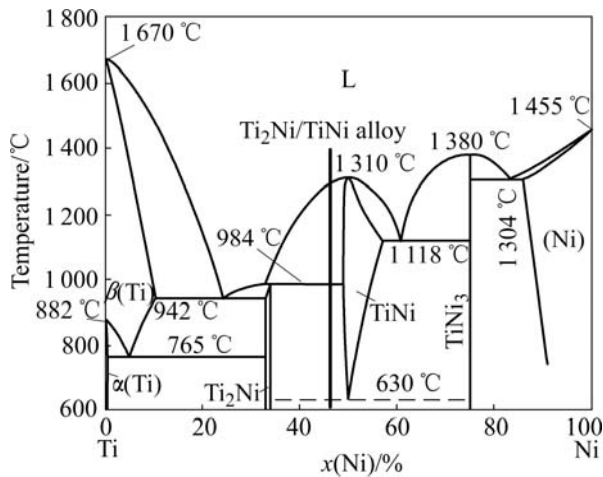


Fig.4 Ti-Ni binary phase diagram

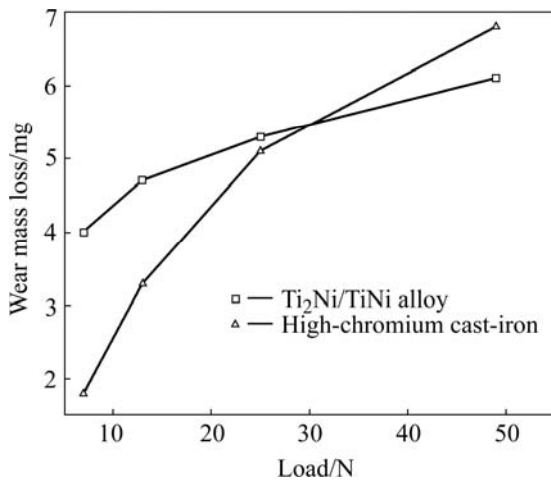


Fig.5 Wear mass loss of Ti₂Ni/TiNi alloy and high-chromium cast iron as a function of load

heavy abrasive wear load of 49 N than the reference material.

The worn surface morphologies of the Ti₂Ni/TiNi alloy and high-chromium cast-iron under test load of 49 N are illustrated in Fig.6. Micro-cutting and plowing grooves are observed on the worn surface of the intermetallic alloy. Minor scaling areas and pits can be observed on the worn surface of the intermetallic alloy. There are plowing grooves and scaling pits on the worn surface of high-chromium cast-iron.

Fig.7 shows that wear debris under test load of 49 N consists of loose powder, flake and silk-like chips. The aforementioned evidence indicates that the dominate wear mechanism of the intermetallic alloy under abrasive wear test is micro-cutting and plowing.

Microstructure of the worn subsurface of the Ti₂Ni/TiNi alloy at a wear test load of 49 N is shown in Fig.8(a). Obvious evidences of fragmentation of the intermetallic Ti₂Ni phase are revealed in the worn

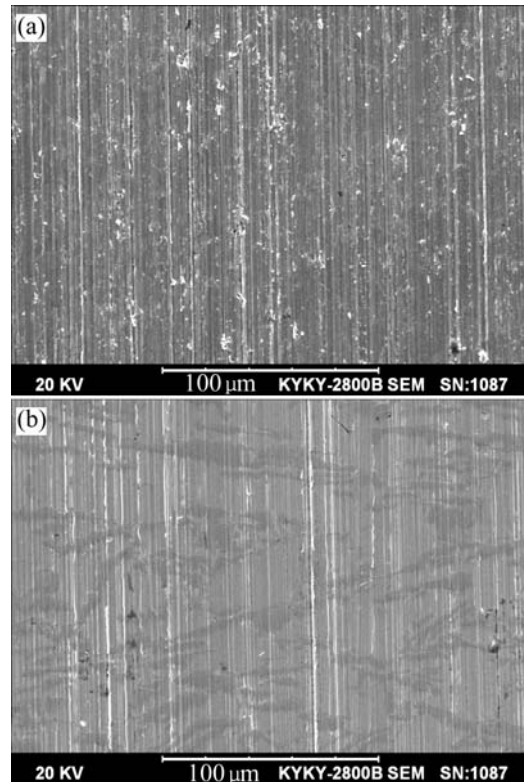


Fig.6 SEM micrographs of worn surface of Ti₂Ni/TiNi alloy (a) and high-chromium cast-iron (b) under wear test load of 49 N

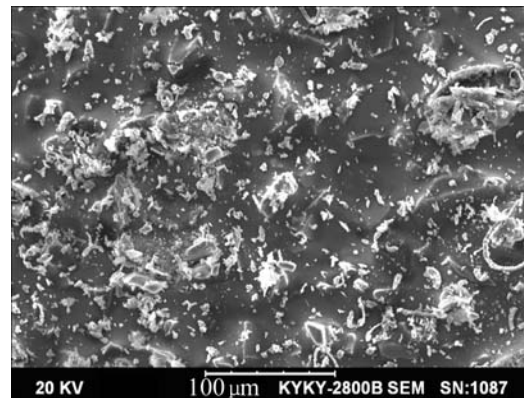


Fig.7 SEM micrograph showing wear debris of Ti₂Ni/TiNi alloy under test load of 49 N

subsurface. However, propagations of cracks initiated from the brittle Ti₂Ni phase are prevented when meeting the ductile TiNi phase. A few cracks contact with each other or grow up, resulting in brittle fracture. Scaling blocks of high-chromium cast-iron are observed on the surface of high-chromium cast-iron, as shown in Fig.8(b).

Fig.9 illustrates the differential scanning calorimetry(DSC) thermogram for Ti₂Ni/TiNi intermetallic alloy. An exothermic peak is observed around 95 °C, corresponding to the temperature of martensitic transformation of TiNi.

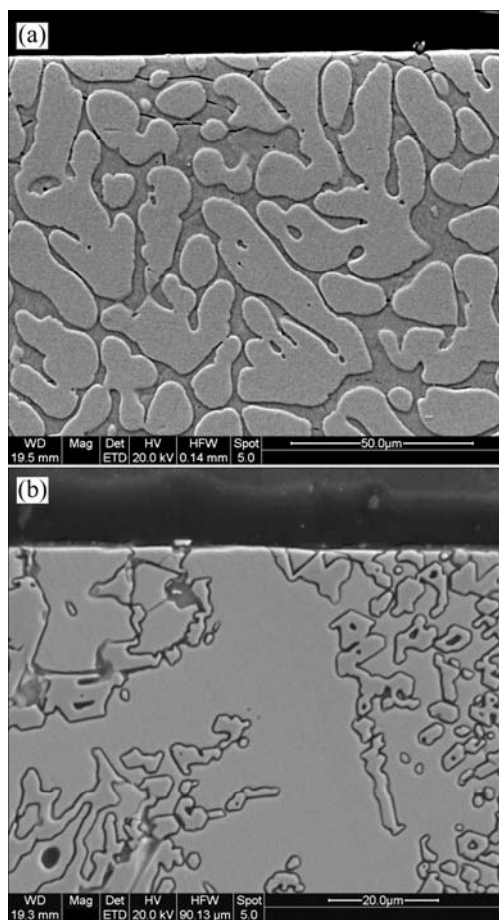


Fig.8 Microstructures of worn subsurface of $Ti_2Ni/TiNi$ alloy (a) and high-chromium cast-iron (b) under wear load of 49 N

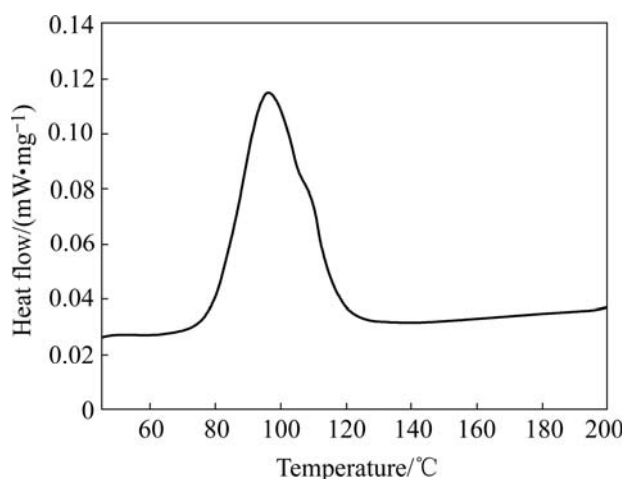


Fig.9 DSC trace from $Ti_2Ni/TiNi$ alloy

XRD results are presented for the worn surface of intermetallic alloy under wear load of 7, 13, 25 and 49 N in Fig.10. The main diffraction peak of plane index (110) of $B2$ $TiNi$ phase becomes broader with the increase of wear load. This indicates the intermetallic alloy that suffers abrasive wear under higher wear load contains more $B2$ $TiNi$ phase.

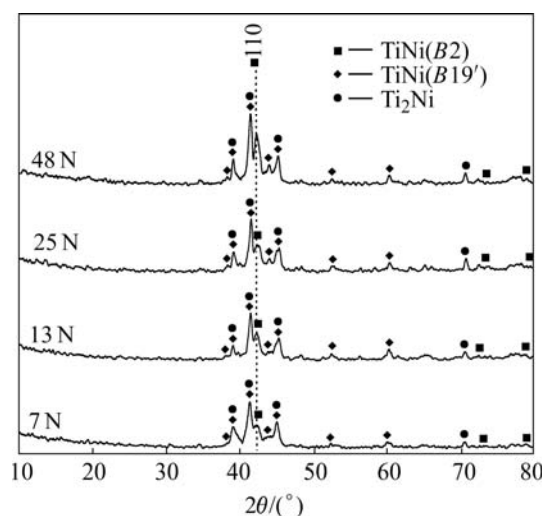


Fig.10 XRD patterns of laser melting/deposited $Ti_2Ni/TiNi$ intermetallic alloy after abrasive wear under different wear loads

4 Discussion

Repeated actions of high contact stress on the worn surface and subsurface are damage to the $Ti_2Ni/TiNi$ alloy. Combination of hard Ti_2Ni and ductility $TiNi$ are attributed to abrasive wear resistance of the intermetallic alloy.

It can be discussed in two sides. On one side, Ti_2Ni of higher hardness strengthens the $Ti_2Ni/TiNi$ alloy resistance to high contact stress. The fresh surface of the $Ti_2Ni/TiNi$ alloy is attacked by cycled contact stress of SiC wear particles. Deformation of $TiNi$ of lower hardness occurs and contact area of abrasive wear increases. Ti_2Ni of high hardness resists more abrasive wear load and protects softer $TiNi$ from further deformation. Cracks initiate in the hard Ti_2Ni due to stress concentration. On the other side, $TiNi$ of excellent ductility improves resistance to brittle fracture of the intermetallic alloy. Cracks of Ti_2Ni phase are prohibited by contacting with each other and scaling with ductility of $TiNi$.

$Ti_2Ni/TiNi$ alloy exhibits better resistance to wear loss under wear load of 49 N and the intermetallic alloy shows better wear resistance because the pseudoelasticity of $TiNi$ improved.

The effect of friction-induced heating effect increases sharply as the abrasive wear process continues. This results in the phenomenon that the temperature of the worn surface and subsurface of the intermetallic alloy is raised. $B19'$ $TiNi$ phase on the worn surface and subsurface of the intermetallic alloy becomes $B2$ $TiNi$ when its temperature is over A_s of $TiNi$ (approximate 95 °C). Then contact stress between the intermetallic alloy

and SiC wear particles induces martensitic transformation ($B2$ TiNi phase $\rightarrow B19'$ phase). Good pseudoelasticity of $B2$ TiNi phase plays an active role in contributing to the wear resistance of the intermetallic alloy.

Fig.11 shows the pseudo-elasticity(PE) and shape memory effect(SME) as function of stress and temperature. Pseudoelasticity area is broader with the increasing of temperature and stress when stress is lower than critical stress (A) that is higher than abrasive wear load of 49 N[1–3]. Owing to higher contact stress and friction-induced heating effect under wear test load of 49 N, the intermetallic alloy after abrasive wear contains more $B2$ TiNi phase, as illustrated in Fig.10. More $B2$ TiNi and better pseudoelasticity of the intermetallic alloy are attributed to preventing from increasing sharply under higher wear test load.

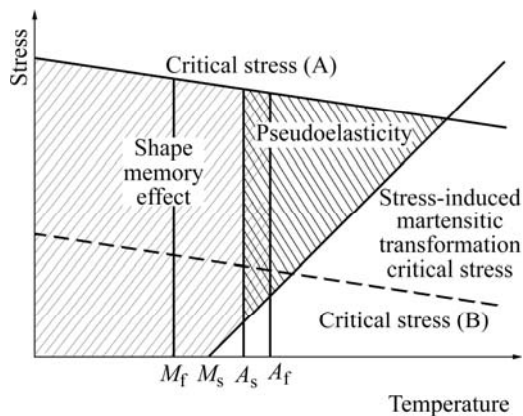


Fig.11 Schematic illustration of pseudo-elasticity(SME) and shape memory effect(PE) as function of stress and temperature

5 Conclusions

1) The laser melting/deposited $Ti_2Ni/TiNi$ intermetallic alloy consists of TiNi primary dendrites and the interdendritic Ti_2Ni continuous matrix.

2) The dominate wear mechanism of the intermetallic alloy and high-chromium cast iron under abrasive wear test is micro-cutting and plowing by hard SiC wear particles.

3) Combination of hard Ti_2Ni and ductile TiNi are attributed to abrasive wear resistance of the intermetallic alloy.

4) Wear mass loss of $Ti_2Ni/TiNi$ alloy increases slowly with the increase of wear load and the alloy shows better wear resistance under wear load of 49 N than high-chromium cast iron due to pseudoelasticity of TiNi.

Acknowledgement

The authors would like to thank ZHANG Ling-yun

and YU Rong-li for their invaluable assistance during the laser melting deposition and the metallographic experiments.

References

- [1] LI D Y, LIU R. The mechanism responsible for high wear resistance of pseudo-elastic TiNi alloy—A novel tribo-material [J]. *Wear*, 1999, 225/229: 777–783.
- [2] LI D Y. Development of novel wear-resistant materials: TiNi-based pseudoelastic tribomaterials [J]. *Mater Des*, 2000, 21: 551–555.
- [3] LI D Y. A new type of wear-resistant material: Pseudo-elastic TiNi alloy [J]. *Wear*, 1981, 221: 116–123.
- [4] SHIDA Y, SUGIMOTO Y. Water jet erosion behaviour of Ti-Ni binary alloys [J]. *Wear*, 1991, 146: 219–228.
- [5] JIN J L, WANG H L. Wear resistance of Ni-Ti alloy [J]. *Acta Metall Sin*, 1988, 24: 66–70. (in Chinese)
- [6] CHENG Y, ZHENG Y F. The corrosion behavior and hemocompatibility of TiNi alloys coated with DLC by plasma based ion implantation [J]. *Surf Coat Technol*, 2006, 200: 4543–4548.
- [7] LIN H C, WU S K, YE H C. A comparison of slurry erosion characteristics of TiNi shape memory alloys and SUS304 stainless steel [J]. *Wear*, 2001, 249: 557–565.
- [8] CHENG X H, LI Z H, XIANG G Q. Dry sliding wear behavior of TiNi alloy processed by equal channel angular extrusion [J]. *Mater Des*, 2007, 28: 2218–2223.
- [9] WU S K, CHEN C C. A study on the machinability of a $Ti_{49.6}Ni_{50.4}$ shape memory alloy [J]. *Mater Lett*, 1999, 40: 27–32.
- [10] WU S K, LEE C Y, LIN H C. A study of vacuum carburization of an equiatomic TiNi shape memory alloy [J]. *Scripta Mater*, 1997, 37: 837–842.
- [11] WANG Y, WANG H M. Wear resistance of laser clad Ti_2Ni_3Si reinforced intermetallic composite coatings on titanium alloy [J]. *Appl Surf Sci*, 2004, 229: 81–86.
- [12] WANG Y, LI A, ZHANG L Y, Wang H M. Microstructure and Wear resistance of laser melted $Ti_5Si_3/NiTi$ intermetallic alloys [J]. *Rare Metal Mat Eng*, 2006, 35: 1967–1970. (in Chinese)
- [13] WANG H M, CAO F, CAI L X, TANG H B, YU R L, ZHANG L Y. Microstructure and tribological properties of laser clad $Ti_2Ni_3Si/NiTi$ intermetallic coatings [J]. *Acta Mater*, 2003, 51: 6319–6327.
- [14] WANG H M, LIU Y F. Microstructure and wear resistance of laser clad $Ti_5Si_3/NiTi_2$ intermetallic composite coating on titanium alloy [J]. *Mater Sci Eng A*, 2002, 338: 126–132.
- [15] YE H Z, LI D Y, EADIE R L. Improvement in wear resistance of TiNi-based composites by hot isostatic pressing [J]. *Mater Sci Eng A*, 2002, 329/331: 750–755.
- [16] WU S K, LIN H C, LEE CY. Gas nitriding of an equiatomic TiNi shape memory alloy (II): Hardness, wear and shape memory ability [J]. *Surf Coat Technol*, 1999, 113: 13–16.
- [17] LIN H C, LIAO H M, HE J L, LIN K M, Chen K C. Wear characteristics of ion-nitrided $Ti_{50}Ni_{50}$ shape memory alloys [J]. *Surf Coat Technol*, 1997, 92: 178–189.
- [18] NAGARAJAN R, CHATTOPADHYAY K. Intermetallic $Ti_2Ni/TiNi$ nanocomposite by rapid solidification [J]. *Acta Metall Mater*, 1994, 42: 947–958.
- [19] LIANG Y N, LI S Z, JIN Y B, JIN W, LI S. Wear behavior of a TiNi alloy [J]. *Wear*, 1996, 198: 236–241.
- [20] JIANG X Y, XU H B, GONG S K. The crystallization kinetics of an amorphous Ti-rich NiTi film [J]. *Acta Metall Sin (English Letters)*, 2000, 13: 1131–1135.
- [21] ISHIDA A, SATO M, MIYAZAKI S. Mechanical properties of Ti-Ni shape memory thin films formed by sputtering [J]. *Mater Sci Eng A*, 1999, 273/275: 754–757.
- [22] WANG H M, ZHANG L Y. Laser smelting furnace with water cooled copper mould and method for melting ingot. CN 02121496.4 [P]. 2002-06-26. (in Chinese)

(Edited by YANG Bing)